01 Jan 2023

Molecular Mechanism Study on the Effect of Nonionic Surfactants with Different Degrees of Ethoxylation on the Wettability of Anthracite

Xuanlai Chen

Guochao Yan

You Zhou

Guang Xu
Missouri University of Science and Technology, guang.xu@mst.edu

et. al. For a complete list of authors, see https://scholarsmine.mst.edu/min_nuceng_facwork/1673

Recommended Citation

X. Chen et al., "Molecular Mechanism Study on the Effect of Nonionic Surfactants with Different Degrees of Ethoxylation on the Wettability of Anthracite," *Chemosphere*, vol. 310, article no. 136902, Elsevier, Jan 2023.
The definitive version is available at https://doi.org/10.1016/j.chemosphere.2022.136902

Chemosphere 310 (2023) 136902

Contents lists available at ScienceDirect

Chemosphere

journal homepage: www.elsevier.com/locate/chemosphere

Molecular mechanism study on the effect of nonionic surfactants with different degrees of ethoxylation on the wettability of anthracite

Xuanlai Chen [a,*], Guochao Yan [b], You Zhou [c,**], Guang Xu [d], Xuyang Bai [b], Jiajun Li [b]

[a] School of Engineering, The University of Western Australia, Perth, WA, 6009, Australia
[b] College of Mining Engineering, Taiyuan University of Technology, Taiyuan, 030024, China
[c] School of Metallurgy and Environment, Central South University, Changsha, 410083, China
[d] Department of Mining Engineering, Missouri University of Science and Technology, Rolla, MO, 65409, USA

HIGHLIGHTS

- A high molecular weight coal model was used to describe the interface properties.
- The wetting mechanism for improving the hydrophilicity of anthracite was uncovered.

GRAPHICAL ABSTRACT

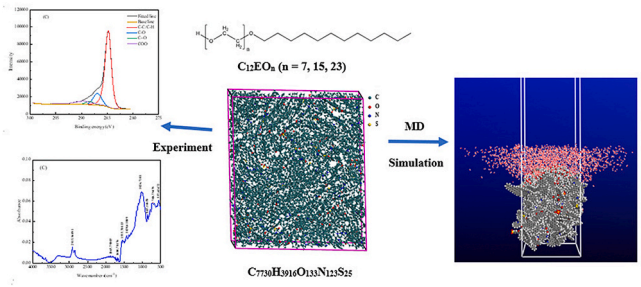

ARTICLE INFO

Keywords:
Anthracite
Wettability
Lauryl polyoxyethylene ether

ABSTRACT

A serious risk to the production safety of coal mines is coal dust. The wettability of coal may be successfully changed by adding surfactants to water. However, the creation of very effective dust suppressants is constrained by the lack of knowledge about the microscopic interaction mechanism between coal dust and surfactants. In this investigation, we explained macroscopic experimental phenomena from a molecular perspective. The lauryl polyoxyethylene ethers (C_{12} $(EO)_n$, n = 7,15,23) were selected. The macromolecular model of anthracite with 55 different components was constructed. Surface tension experiments and hydrophilic lipophilic balance (HLB) calculations showed that the ability of surface hydrophilicization followed the order of C_{12} $(EO)_7$<C_{12} $(EO)_{15}$<C_{12} $(EO)_{23}$. Contact angle experiment, XPS and FTIR experiments proved that after the surfactants were adsorbed on the surface of anthracite, the content of carbon element decreased and the content of oxygen element increased, indicating the enhanced surface hydrophilicity. The simulation results showed that with the degree of ethoxylation increases, the adsorption strength of surfactants becomes stronger, and the hydrophilic head group of surfactant on anthracite surface is more uniformly distributed. The greater the degree of ethoxylation, the more powerfully the modified coal surface can bind to water molecules.

* Corresponding author.
** Corresponding author.
E-mail addresses: chenxuanlai0948@outlook.com (X. Chen), zhouyou2010@csu.edu.cn (Y. Zhou).

https://doi.org/10.1016/j.chemosphere.2022.136902
Received 12 August 2022; Received in revised form 26 September 2022; Accepted 13 October 2022
Available online 17 October 2022

1. Introduction

A serious risk to the production safety of coal mines is coal dust. There is coal mine dust in the air or on the roadways, which not only makes it harder to see but also pollutes the environment. Coal seam spraying is a common method used today to reduce coal dust, which is crucial for the productivity and safety of coal mines (Ni et al., 2019a; Zhou and Qin, 2021). However, due to the strong hydrophobicity of the anthracite surface, the efficiency of using water alone for anthracite dust reduction is far from satisfactory (Ni et al., 2019b; Xu et al., 2018).

The structure of surfactants contains both hydrophobic and hydrophilic groups, which allows them to efficiently alter the characteristics of the coal surface. The wettability of coal dust may be dramatically altered by the little addition of surfactant to water (Chang et al., 2020), and the surfactants mainly change the wettability of coal by affecting the hydrophobicity and hydrophilicity of the coal surface (Xu et al., 2018). It was found that the coal surface became more hydrophobic after being adsorbed by the surfactant (Mishra and Panda, 2005). Different surfactant structures and their effects on coal wettability have been reported by many researchers (Guo et al., 2018; Liu et al., 2020a, 2020b; Xu et al., 2019; Yao et al., 2017).

In recent years, researchers worldwide have carried out a large number of experimental studies on surfactants changing coal wettability (Li et al., 2020a; Lyu et al., 2019; Ni et al., 2019b; Yao et al., 2017; Yuan et al., 2020). The structure, kinetics, and energy properties of the molecular adsorption process on mineral surfaces were seldom discussed, and empirical research only produced macroscopic results. More academics are turning to molecular dynamics modeling to analyze the change in coal wettability from a microscopic viewpoint (Guo et al., 2018; Liu et al., 2020b; You et al., 2019; Zhang et al., 2020). However, most coal models selected for the research were single-component coal models in the current research on the properties of coal interface with molecular dynamics (Chen et al., 2020; Guo et al., 2018; Li et al., 2020b; Liu et al., 2020b; Xia et al., 2019; You et al., 2018, 2019; Yuan et al., 2020; Zhang et al., 2017, 2020). The molecular weight of this form of coal model is low, and although it may approximate coal's features to some degree, it is far from accurate. Coal is a complex multi-component macromolecular organic matter, so the single-component and small-molecular-weight coal model used in the current research is still far from the real situation. A large-molecular-weight Jincheng anthracite model ($C_{7730}H_{3916}O_{133}N_{123}S_{25}$) composed of 55 different components through a large number of experiments in the early stage was proposed (Yan et al., 2020). This model was utilized to analyze the interface features since it was more accurate in terms of the molecular weight and richness of the coal model's components. The macromolecular coal model has a significant drawback in that it uses more computational resources and takes longer to compute.

The current research on coal interface characteristics is focused on low-rank coal, while there is little research on the interface characteristics of high-rank coal. There is currently minimal study on the interface features of high-rank coal, with the majority of studies focusing on low-rank coal. This is a new investigation on coal's interfacial characteristics utilizing a multicomponent, high molecular weight coal model that is more accurate.

In this investigation, the Jincheng anthracite model ($C_{7730}H_{3916}O_{133}N_{123}S_{25}$) (Yan et al., 2020) with 55 components and a large molecular weight will be selected. The effects of three surfactants $C_{12}EO_n$ (n = 7, 15, 23) with different degrees of ethoxylation on the wettability of anthracite will be investigated by experiments and molecular dynamics (MD) simulations. First, surface tension tests and HLB calculations will be used to evaluate the hydrophilicity of three surfactants. The capacity of surfactants to alter the wettability of anthracite will be compared from the standpoint of surface element alterations using XPS and FTIR analyses. Second, molecular simulations will be used to explain macroscopic experimental phenomena, by measuring adsorption energy, contact surface area (CSA), diffusion cofficient, radial distribution function (RDF), and number of hydrogen bonds.

2. Experiments and simulations

2.1. Materials

The anthracite from Zhaozhuang Coal Mine, Jincheng, Shanxi Province, China was selected as the experimental coal sample, and coal samples with a particle size ranging from 200 to 300 mesh (pore diameter 0.074 mm–0.050 mm) were selected by crushing and screening. In order to further reduce the influence of inorganic minerals in coal, HCl–HF–HCl acid elution of minerals was carried out. and washed in excess distilled water until the pH of the filtrate was neutral. The ash content on dry basis after the treatment was 0.3%.

The main chemicals used in this research were $C_{12}EO_n$ (n = 7, 15, 23; purity >98%), which were obtained from the Nanjing Ruichuang Chemical Technology Co., Ltd. The structure of the polyoxyethylene ether is shown in the support material Fig. 1S. HLB value of surfactant can reflect its hydrophilic ability, and it was calculated according to the Griffin's method (Lin et al., 2017; Liu et al., 2018; Rodriguez-Abreu, 2019). The HLB was defined by Eq. (1).

$$HLB = 20\ M_H / (M_H + M_L) \quad (1)$$

where M_H is the molecular weight of hydrophilic head of surfactant molecule, g/mol; M_L is the molecular weight of hydrophobic end of surfactant molecule, g/mol. The obtained HLB values of C_{12} $(EO)_n$ (n = 7, 15, 23) are 12.49, 15.62, and 16.90 respectively.

2.2. Experiment

2.2.1. Surfactant adsorption

Before the follow-up experiment, it was necessary to carry out an adsorption test on the coal sample after pickling, so that the surfactant was adsorbed on the surface of anthracite, and the concentration of different types of surfactant solution was 200 mg/L. When the concentration of C_{12} $(EO)_n$ surfactant solution is 200 mg/L, it is higher than the critical micelle concentration (CMC) of each surfactant, and when the concentration of surfactant is above CMC, the wetting effect is the best (Liu et al., 2018). 500 mg acid-washed coal sample was mixed with 500 mL of surfactant solution, and the solution was placed in a water bath with a magnetic stirring device and stirred at a constant speed (800 r/min) for 10 h at room temperature. The solution was centrifuged in a centrifuge (2000 r/min, 30 min), the obtained coal sample was vacuum filtered three times, and the residual surfactant solution in the coal was washed with DI water.

2.2.2. Surface tension measurements

The surface tension values of the above three nonionic surfactant monomer solutions were measured by Dataphysics DCAT21 surface tensiometer. The measuring range was 1–2000 mN/m, the sensitivity was ±0.001 mN/m, the mass range of the balance was 10 μg–210 g, and the experimental temperature was 25 °C.

2.2.3. Contact angle measuring

The JY-82C contact angle measuring device was used for the contact angle test. We examined the coal samples' contact angles with four liquids (C_{12} $(EO)_7$, C_{12} $(EO)_{15}$, C_{12} $(EO)_{23}$, and deionized water). The test liquid was swirled for 24 h to remove the impact of air bubbles before the coal sample was compressed using the pulverised coal method. Each test was administered three times, with the average being used.

2.2.4. XPS measurements

XPS experiments were performed using a Thermo Scientific K-Alpha X-ray electron spectrometer, and a monochromatic Al target (K_α $h\nu$ = 1486.6 eV) was used as the X-ray source. During the test, the vacuum

degree of the analysis chamber is better than 5.0 E-7mBar. The full-spectrum scan pass energy was 100 eV, and the resolution of the measurement scan was 1 eV. The narrow-spectrum scan was performed for 5 cycles of signal accumulation (different scan times for different elements), the pass energy was 50 eV, and the step size was 0.05 eV, which was used for the scan of C 1s. The binding energy was charge-corrected for the spectrum by contaminating carbon (C 1s = 284.8 eV). Background effects were subtracted using Shirley's method.

2.2.5. FTIR measurements

FTIR measurements were performed using a Thermo Scientific Nicolet model iS20 Fourier Transform Infrared Spectrometer. Before the experiment, the adsorbed sample and KBr solid powder were mixed and dried in a vacuum drying oven to remove moisture to exclude the influence of moisture on the infrared test. Before the experiment, the adsorbed samples and KBr solid powder were dried in a vacuum drying oven respectively to exclude the influence of moisture on the FTIR test. 2 mg of the adsorbed sample and 200 mg of pure KBr were ground evenly in a ratio of 1:100, placed in a mold, and pressed into a transparent sheet on a powder tablet machine at a pressure of 10 MPa. The wavenumber range was 4000–400 cm^{-1}, the number of scans was 32, the resolution was 4 cm^{-1}, and the moving mirror speed was 0.4747.

2.3. Modeling study

The unit cell size of the anthracite model is 5.4 × 4.8 × 5.5 nm^3 (X Y Z), and the model density is 1.43 g/cm^3. The surfactant layer contains 10 molecules and the water layer contains 2000 molecules. Molecular dynamics simulations were performed in Materials Studio 8.0. The COMPASS force field was selected to describe the intermolecular interactions. Before the MD simulation, the energy of all models was minimized using the Smart algorithm. Subsequently, NVT ensemble was used for MD simulation. The nose was used for thermostat (Zhang et al., 2020). The time step was set to 1 fs The temperature was 298 K. In all MD simulations, the Ewald algorithm was selected for long-range electrostatic interaction, and the accuracy was 0.001 kcal/mol, and the atom-based algorithm was selected for the van der Waals interaction, and the cut-off distance was 1.25 nm. A 8 nm vacuum layer was added to the surface of each model to eliminate the mirror effect.

As shown in Fig. 1, the interaction of water, surfactant, and anthracite was studied in two stages during the MD simulation. Adsorption of surfactant and anthracite was the initial step, which allowed for the analysis of the microscopic structure and energy of the two substances' adsorption processes. At this point, a surfactant layer was applied using the build layer tool to the anthracite surface, and then a 1000 ps MD simulation was run using the NVT ensemble. The second step, which may be utilized to analyze the change in surface wettability of surfactant-modified anthracite, is the interaction between water molecules and the modified anthracite's surface. At this point, a 500 ps MD simulation was run. MD simulations of water-anthracite were also run as a comparison. The unit cell boundary was concealed to better display the adsorption conformation. Adsorption process of surfactant on anthracite (B) C_{12} $(EO)_{15}$; (C) C_{12} $(EO)_{23}$ is showed in Fig. 2S.

3. Results and discussion

3.1. Experiments analysis

3.1.1. Surface tension experiment

An essential assessment metric for surfactant effectiveness is surface tension. Due to its high surface tension, clean water has a low capacity to moisten coal dust. Surfactants may successfully lower the surface tension of an aqueous solution and increasing wetting effectiveness (Xu et al., 2018).

The wetting effect on coal dust is best when the concentration of surfactant is above the critical micelle concentration (CMC) (Liu et al., 2018). For polyoxyethylene nonionic surfactants, the critical micelle concentration (CMC) increases when the degree of ethoxylation increases. According to literature data, the concentration of C_{12} $(EO)_n$ series surfactant solution is higher than CMC when the concentration is 200 mg/L (Li et al., 2019; Liu et al., 2018; Rodriguez-Abreu, 2019). In this experiment, the concentration of 3 kinds of surfactant solutions was selected as 200 mg/L. The surface tension results are shown in Table 1, The fluctuation range is 0.5–1.5 (mN/m).

The surface tension values of the three surfactants are ranked as C_{12} $(EO)_7$<C_{12} $(EO)_{15}$<C_{12} $(EO)_{23}$. This is because the greater the number of polyoxyethylenes, the stronger the polarity of the surfactant molecule, resulting in a stronger interaction with water molecules. The degree of size and force balance between the hydrophilic and hydrophobic groups in the surfactant is expressed by a number called the hydrophilic-lipophilic balance (HLB). The strength of the surfactant's hydrophilicity and hydrophobicity are inversely correlated with its HLB value. The order of HLB values of the three surfactants is C_{12} $(EO)_7$ (12.49) < C_{12} $(EO)_{15}$ (15.62) < C_{12} $(EO)_{23}$ (16.9). This is consistent with the conclusion of surface tension, indicating that C_{12} $(EO)_{23}$ has the strongest hydrophilicity. The hydrophilicity of C_{12} $(EO)_7$ is the weakest.

3.1.2. Contact angle measuring

The contact angle test measures how well the surfactant solution wets the anthracite surface by measuring the change in contact angle value. The contact angle values produced with anthracite for the same concentration (200 mg/L) of surfactant solutions (C_{12} $(EO)_7$, C_{12} $(EO)_{15}$, and C_{12} $(EO)_{23}$) were measured. Contact angle data of deionized water and coal sample was employed as the control group. The contact angle values at 1s time were selected for comparison, as shown in Fig. 2 (A). The measured contact angle between deionized water and anthracite is

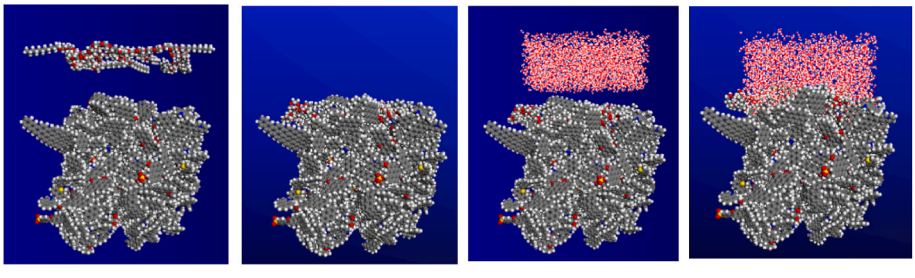

Fig. 1. Adsorption process of surfactant on anthracite (A) C_{12} $(EO)_7$. (a) was the first Stage initial conformation, (b) was the first stage final equilibrium conformation, (c) was the second-stage initial conformations, and (d) was the second-stage equilibrium conformations.

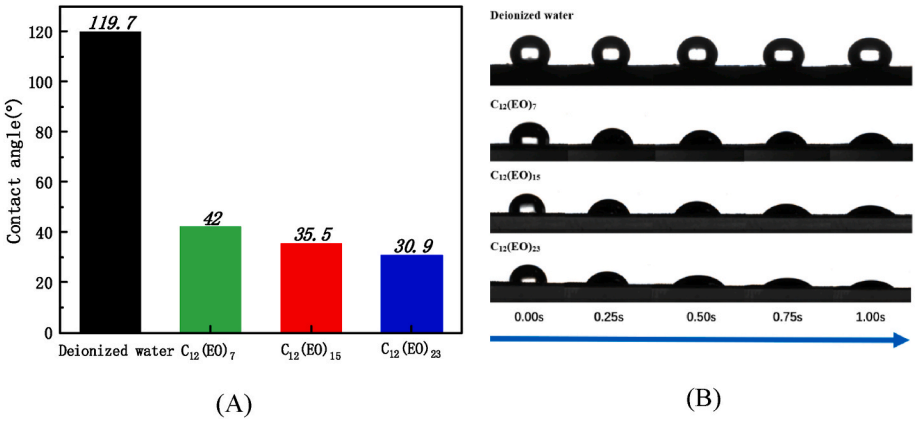

Fig. 2. Contact angle experimental data (A) contact angle at 1s; (B) dynamic change of contact angle.

119.7°, the contact angle between C_{12} $(EO)_7$ and anthracite is 42°, the contact angle between C_{12} $(EO)_{15}$ and anthracite is 35.5°, and the contact angle between C_{12} $(EO)_{23}$ and anthracite is 30.9°. It can be found from Fig. 2 (B) that the diffusion of surfactant solution on the surface of coal sample is a dynamic process. The order of the ability to reduce the contact angle during the wetting of coal dust is: C_{12} $(EO)_{23}$>C_{12} $(EO)_{20}$>C_{12} $(EO)_7$. Through the contact angle test, it was found that the wettability of anthracite coal can be effectively improved after adding surfactants in water, and the order of the ability to improve the wettability of anthracite is: C_{12} $(EO)_{23}$>C_{12} $(EO)_{20}$>C_{12} $(EO)_7$.

For an ideal solid-liquid system, the rate of change of diffusion and permeation with time can be expressed by Eq. (2). In this formula, K is generally defined as the diffusion-permeation constant. The larger the K value, the higher the efficiency of the surfactant wetting the coal dust.

$$\frac{d\theta}{dt} = -K\theta \tag{2}$$

When the permeation and diffusion tend to 0, Eq. (3) can be obtained by adding a constraint to the above formula.

$$\frac{d\theta}{dt} = -K\theta\left(1 - \frac{\theta i - \theta}{\theta i - \theta e}\right) \tag{3}$$

Arranging the above formula and integrating it can get Eq. (4).

$$K = \frac{(\theta_e - \theta_i)}{t\theta_e} \ln\left(\frac{\theta_i(1-\theta) - \theta_e}{\theta(\theta_e - \theta_i)}\right) \tag{4}$$

To fit a nonlinear curve to the wetting process of coal dust, utilise Eq. (4). Fig. 3S displays the fitting curve, and Table 1S displays the fitting equation and parameters. It can be found from the table that when deionized water wets the coal flakes, its K value is 0.01072; after adding surfactant, the wetting parameter K value increases rapidly, the K value of C_{12} $(EO)_7$ is 2.00949, and C_{12} $(EO)_{15}$ has a K value of 2.18237 and C_{12} $(EO)_{23}$ has a K value of 3.34998. According to the K value, it shows that the order of diffusion and penetration ability on the surface of anthracite is: C_{12} $(EO)_{23}$>C_{12} $(EO)_{15}$>C_{12} $(EO)_7$.

3.1.3. XPS experiment

As shown in Table 2 and Fig. 4S, distinct carbon and oxygen peaks appeared in the XPS spectrum, which were the main components after the surfactant adsorbed on the coal surface. After the adsorption of different surfactants, the carbon and oxygen contents on the coal surface were significantly different.

The quantitative peak analysis method can visually display the existence status of each element. The results are shown in the support material.

The order of carbon element content is Raw coal > C_{12} $(EO)_7$> C_{12} $(EO)_{15}$> C_{12} $(EO)_{23}$, and the order of oxygen element content is Raw coal < C_{12} $(EO)_7$< C_{12} $(EO)_{15}$< C_{12} $(EO)_{23}$. This shows that after adsorption of surfactant, the surface hydrophilicity of anthracite is enhanced. C_{12} $(EO)_{23}$ has the best effect on enhancing the wettability of anthracite, and the modified coal surface has the best hydrophilicity. And C_{12} $(EO)_7$ has the worst effect on enhancing the wettability of anthracite. According to the difference in the binding energy of electrons in the inner layer of atoms, the C 1s peak area was further fitted by peaks, and the curve was obtained as shown in Fig. 5S and Table 3.

First compare the adsorption of three surfactants, from Fig. 5S and Table 3, the C 1s peak area and proportion show that after adsorption of C_{12} $(EO)_{23}$, the C–C/C–H content on the coal surface is the lowest, only 73.09%, the oxygen-containing functional group content is relatively high, accounting for 26.9%. This phenomenon shows that C_{12} $(EO)_{23}$ has the most significant enhancement effect on the wettability of anthracite. In terms of the proportion of oxygen-containing functional groups, there is little difference in the proportion of C–O on the surface of modified coal, but the proportion of C═O and COO after C_{12} $(EO)_{23}$ adsorption is the highest. These two oxygen-containing functional groups are derived from anthracite. This shows that during the adsorption process. C_{12} $(EO)_{23}$ tends to cover the hydrophobic sites on the anthracite surface, and a small amount of hydrophilic functional groups on the anthracite surface are still exposed to air.

Additional comparisons between the C1s peaks of raw coal and modified coal surfaces. The ratio of C–C/C–H after adsorption is larger than that of raw coal because the surfactant includes a significant proportion of C–C/C–H. Following the surfactant's adsorption, the coal's surface had a much lower ratio of C═O and a little higher ratio of COO. Anthracite was the source for both functional groupings. This demonstrates that whereas COO is more exposed to the air and is not covered, surfactant will preferentially adsorb on and cover the C═O on the coal surface.

Table 1
Surface tension values of the C_{12} $(EO)_n$ series surfactants and H_2O.

Reagent	N	Surface tension (mN/m)
H_2O	/	71.558
C_{12} $(EO)_7$	7	30.594
C_{12} $(EO)_{15}$	15	33.899
C_{12} $(EO)_{23}$	23	39.740

3.1.4. FTIR experiment

Fourier transform infrared spectroscopy (FTIR) was used to analyze the distribution of surfactants on the surface of anthracite. The FTIR spectrum is shown in the support material.

The FTIR curve of anthracite following surfactant adsorption manifested several peaks, as illustrated in Fig. 6S (A). The vibrational region of aliphatic hydrocarbons is where the peaks between 2950 and 2100 cm^{-1} are located (Chen et al., 2011; Pan et al., 2013). Compared with

Table 2
The relative content of the atomic number of the main elements (except H) on the surface of anthracite after adsorption.

Types	C_{12} $(EO)_7$		C_{12} $(EO)_{15}$		C_{12} $(EO)_{23}$		Raw coal	
	Intensity	PR (%)	Intensity	PR (%)	Intensity	PR (%)	Intensity	PR (%)
C	239,140	84.13	227,337	82.73	200,444	80.53	191,764	86.56
O	99,693	14.02	119,757	15.68	130,701	18.27	91704.4	13.44

Table 3
Peak positions, areas and atomic assignments of C 1s on the surface of anthracite after adsorption.

Groups	C_{12} $(EO)_7$		C_{12} $(EO)_{15}$		C_{12} $(EO)_{23}$		Raw coal	
	Binding energy (eV)	PR (%)	Binding energy (eV)	PR (%)	Binding energy (eV)	PR (%)	Binding energy (eV)	PR (%)
C–C/C–H	284.80	76.00	284.80	75.28	284.80	73.09	284.80	57.66
C–O	286.52	13.24	286.80	14.18	286.91	13.74	285.31	16.38
C=O	285.41	1.86	288.82	2.20	288.41	3.64	286.65	22.51
COO	289.73	8.90	290.28	8.34	289.50	9.52	290.15	3.45

the raw coal surface, the surface of the coal after adsorbing the surfactant is greatly increased in hydrophilicity. After anthracite has absorbed three surfactants, two distinct peaks in the 2950–2100 cm^{-1} range may be seen in Fig. 6S (B). The asymmetric stretching vibration of $–CH_3$, the symmetrical stretching vibration of $–CH_2$, and the asymmetric stretching vibration in aliphatic hydrocarbons often occur near the peak location. It is obvious that when the degree of ethoxylation is increased, the peak diminishes, suggesting a reduction in the hydrophobic $–CH_3$ and $–CH_2$ functional groups, a weakening of coal's hydrophobicity, and an increase in its hydrophilicity.

3.2. Simulation results

3.2.1. Adsorption energy

When two materials are adsorbed, the adsorption energy value is used to calculate the strength of the adsorption. More energy is produced during the adsorption process of the two materials the more negative the adsorption energy is, leading to a larger adsorption strength of the two components (Anvari et al., 2018; Li et al., 2017, 2021). The adsorption energy is defined by Eq. (5)-(7).

$$EV = EV_{total} - EV_A - EV_B \tag{5}$$

$$EE = EE_{total} - EE_A - EE_B \tag{6}$$

$$E = EV + EL \tag{7}$$

where EV stands for van der Waals adsorption energy, EE stands for electrostatic adsorption energy, E stands for total adsorption energy, E_{total} represents the total energy after the adsorption of the two materials is completed, E_A represents the energy of material A, and E_B represents the energy of material B.

First, the adsorption energy of the surfactant when adsorbed to the coal surface was calculated to compare the adsorption strength. Here A stands for surfactant and B for anthracite. The calculated adsorption energy data are shown in the support material.

From the total adsorption energy data of Table 2S, it can be seen that in the process of adsorption, C_{12} $(EO)_n$, n = 7, 15, 23, with the increase of n, the adsorption energy becomes larger. After C_{12} $(EO)_{23}$ adsorbed anthracite, it releases the most energy, the adsorption configuration is the most stable, and the network structure formed is the densest.

Further examination of the van der Waals adsorption energy and electrostatic adsorption energy reveals that the van der Waals adsorption energy makes up around 90% of the adsorption process while electrostatic adsorption energy makes up just 10%. van der Waals interactions dominate the adsorption process. Anthracite is a kind of high-rank coal with few oxygen-containing functional groups on its surface, resulting in a small negative charge on its surface (Lyu et al., 2019). The anthracite and surfactant molecules have few charged atoms, a minor charge difference, and little electrostatic interaction between their negatively and positively charged components. Because of this, the electrostatic adsorption process hardly benefits from the energy. Note that despite the electrical neutrality of nonionic surfactant molecules, their atoms still carry charges.

The water-raw coal and water-modified coal adsorption energies were then calculated to analyze the changes in anthracite wettability.

Comparing the total adsorption energies of the three surfactant systems in Table 3S, it can be found that C_{12} $(EO)_n$, n = 7, 15, 23, as n increases, the adsorption energy becomes larger, and the surface hydrophilicity of the modified coal becomes stronger. This is due to the fact that when the value of n rises, the surface of the modified coal contains more oxygen atoms, which causes the surface to form more hydrogen bonds with water molecules and raises the adsorption force, which releases more energy. This is in line with the findings of the subsequent examination of hydrogen bond numbers. After C_{12} $(EO)_{15}$, C_{12} $(EO)_{23}$ adsorption, the total adsorption energy of the anthracite surface and water increases when compared. It demonstrates that the hydrophilicity of the anthracite surface can be increased by the use of such nonionic surfactants.

Further investigation of the van der Waals adsorption energy and electrostatic adsorption energy reveals that the van der Waals interaction is stronger when water is directly adsorbed on the surface of anthracite, with the van der Waals adsorption energy accounting for approximately 68 percent and the electrostatic adsorption energy accounting for approximately 32 percent. The percentage of electrostatic adsorption energy, however, rose following surfactant modification and reached roughly 57 percent of the overall adsorption energy, exceeding the fraction of van der Waals adsorption energy. It demonstrates that when the changed coal surface adsorbs water, the electrostatic effect is greater. This is due to the fact that the adsorption of such surfactants is akin to coating the hydrophobic anthracite surface with hydrophilic polar oxygen atoms, which strengthens the anthracite's surface polarity and increases the amount of electrostatic adsorption energy. This demonstrates that the polarity of the anthracite surface can be significantly boosted once such non-ionic surfactant are adsorbed on it, strengthening the electrostatic contact and improving the ability to adsorb water molecules.

3.2.2. Contact surface area

The contact surface area (CSA) can reflect the strength of adsorption between two materials. The contact surface area is positively correlated with the adsorption strength. CSA can be defined by Eq. (8).

$$\mathrm{CSA} = \left(\mathrm{SASA}_{\mathrm{anthracite}} + \mathrm{SASA}_{\mathrm{surfactant}} - \mathrm{SASA}_{\mathrm{total}}\right) / 2 \tag{8}$$

where $SASA_{anthracite}$, $SASA_{surfactent}$, and $SASA_{total}$ are the solvent

accessible surface area (SASA) of the anthracite model, the surfactant, and the anthracite-surfactant binary model, respectively. In this study, the applicable probe radius was 0.14 nm (Li et al., 2019). The calculation results of CSA are presented in Fig. 7S.

The CSA values of C_{12} $(EO)_7$, C_{12} $(EO)_{15}$, and C_{12} $(EO)_{23}$ were 31.04 nm^2, 48.05 nm^2, and 70.56 nm^2, respectively. The CSA value of C_{12} $(EO)_{23}$ is the largest, indicating that it has the highest adsorption strength with anthracite. The adsorption strength of C_{12} $(EO)_7$ was the lowest. The adsorption strength conclusion obtained from the CSA analysis is consistent with the adsorption energy analysis above.

3.2.3. Relative concentration distribution

The ability to quantitatively reflect the adsorption capacity and observe the structure of the adsorption layer was achieved by calculating the relative concentration distribution of each component in the ternary system along the Z-axis. The relative concentration distributions of different systems along the Z axis are shown in Fig. 3.

Because a multi-component, high molecular weight coal model was used, the coal model's height in the Z-axis direction surpasses 7 nm. The water layer starts at 5.3 nm when no surfactant is introduced (the starting point is the abscissa value corresponding to the relative concentration when the relative concentration reaches 0.1). After the addition of C_{12} $(EO)_7$, C_{12} $(EO)_{15}$, and C_{12} $(EO)_{23}$, the starting point of the water layer becomes 5.6 nm, 5.9 nm, and 6.6 nm. After the surfactant is added, it is seen that the water layer recedes in the Z-axis direction. The water layer's starting point moves further behind as n gets bigger. This is due to the fact that the surfactant layer creates a network structure that covers the coal surface; the denser the network structure is, and the greater the modification impact is, the bigger the n value. The relative concentration curve peaks of the hydrophilic head groups of the surfactants diminish as the value of n rises. The peak value of the hydrophilic head group curve of C_{12} $(EO)_7$ is about 22, the peak of C_{12} $(EO)_{15}$ curve is about 16, and the peak of C_{12} $(EO)_{23}$ is about 13. The three surfactants' hydrophilic head group distribution widths are all about 2.4 nm. This demonstrates that when n grows, the degree of aggregation of the hydrophilic headgroups at a single position reduces, resulting in a more uniform distribution over the whole distribution range. This facilitates the penetration and adsorption of water molecules. The C_{12} $(EO)_7$ hydrophobic alkyl tail chain shows a single peak at 6.9 nm with a peak of 14.4. C_{12} $(EO)_{15}$ has double peaks at 6.9 nm and 7.6 nm, both peaks are about 11. C_{12} $(EO)_{23}$ appeared three peaks at 6.5 nm, 7 nm, and 7.5 nm, and the peaks were 9.2, 11, and 9 in turn. The number of peaks rises and the peak value falls as n grows, demonstrating a more equal distribution over the distribution range. C_{12} $(EO)_{23}$ has the greatest modifying impact on anthracite because its peak at 6.5 nm is closest to the coal's surface. Although there is a hydrophobic interaction between the hydrophobic alkyl tail chain and the anthracite's aromatic structure, as n grows, the hydrophilic head group's interaction with water becomes stronger and eventually takes control. As a consequence, in addition to the uniform distribution of the hydrophilic head groups, the distribution of the hydrophobic tails is also compelled to be uniform.

3.2.4. Diffusion cofficient

The adsorption of surfactants to anthracite can affect the dynamic behavior of water molecules. The diffusion coefficient of water molecules were calculated to analyze the effect of surfactants on the aggre-

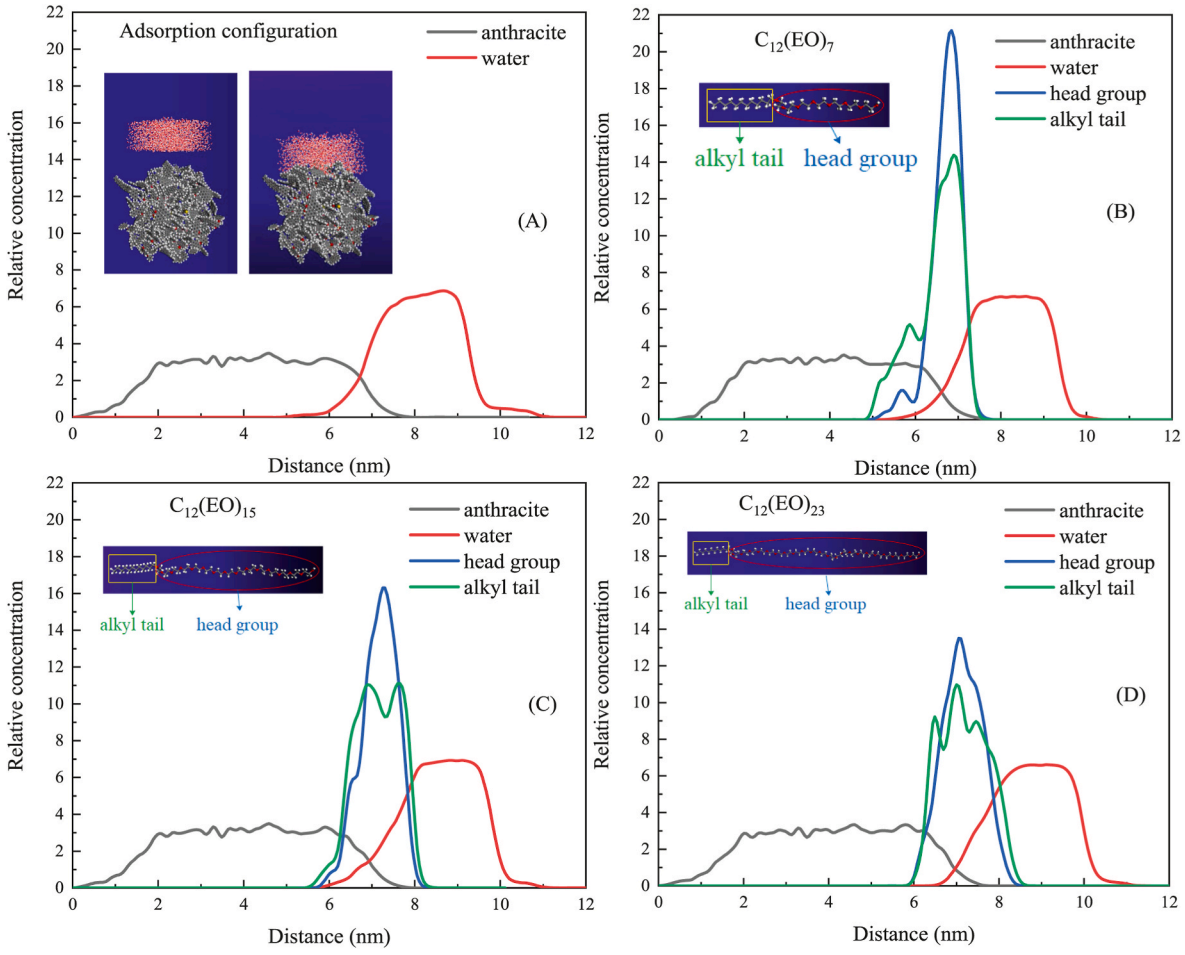

Fig. 3. Relative concentration distribution along the Z axis (A) water-anthracite system; (B) water-C_{12} $(EO)_7$-anthracite system; (C) water-C_{12} $(EO)_{15}$-anthracite system; (D) water-C_{12} $(EO)_{23}$-anthracite system.

gation properties of water molecules. It is determined using Eq. (9).

$$D = \lim_{t\to\infty}\left(\frac{MSD}{6t}\right) = \frac{1}{6}K \tag{9}$$

K represents the slope of the MSD curve, and 1/6 of the slope is the diffusion coefficient.

The diffusion coefficient when water is directly adsorbed to anthracite is 6.4 × 10^{-9} m^2/s. The diffusion coefficient after adding C_{12} $(EO)_7$ is 5.69 × 10^{-9} m^2/s, the diffusion coefficient after adding C_{12} $(EO)_{15}$ is 5.31 × 10^{-9} m^2/s, and the diffusion coefficient after adding C_{12} $(EO)_{23}$ is 5.21 × 10^{-9} m^2/s. Surfactants were added, and this dramatically reduced the diffusion coefficient. It demonstrates how the presence of surfactant reduces the water molecules' capacity for free diffusion. This is because the polar oxygen atoms in the ethoxy hydrophilic group and the water molecules create hydrogen bonds, which prevent the water molecules from freely diffusing. The diffusion coefficient is less the more ethoxylation there is. This is because the more the number of ethoxy groups, the more polar oxygen atoms on the surface of the modified coal, the stronger the polarity of the surface, and the stronger the ability to bind water molecules. According to the diffusion coefficient analyses shown above, adding these surfactants enhances the anthracite surface's hydrophilicity, and the more ethoxylation is present, the more hydrophilic the surface of modified coal is. This agrees with the study of hydrogen bond numbers below.

3.2.5. Radial distribution function

The coordination number may be used to assess the degree of aggregation of B atoms surrounding A atoms as determined by the radial distribution function (RDF) between atoms. The radial distribution function's initial peak, which is high and sharp, shows that both the order and the interaction between the atoms are strong. (He et al., 2010; Yan et al., 2011; Yang et al., 2011; Zhao et al., 2010). RDF is defined by Eq. (10).

$$g(r) = \frac{1}{4\pi\rho_B r^2}\cdot\frac{dN}{dr} \tag{10}$$

In the formula, r represents the distance between B atoms and A atoms; ρ_B represents the density of B atoms; dN is the average number of B atoms in the range from r to r + dr (A is the reference atom).

First, the RDF between the oxygen atom in the surfactant ethoxy group (O_S) and the hydrogen atom in the water (H_W) was calculated. The RDF result is shown in Fig. 4 (A).

As the degree of ethoxylation increases, the first peak of O_S-H_W gradually decreases. As the value of n increases, the aggregation degree of water molecules around a single oxygen atom in the ethoxy group weakens. However, it is considered that as the value of n increases, the number of oxygen atoms increases. Therefore, in general, the higher the degree of ethoxylation, the stronger the binding ability of a single surfactant molecule to water molecules.

The coordination number was further calculated, and the above conclusion was quantified. The larger the coordination number, the stronger the interaction between atoms. The coordination number was calculated by the following Eq. (11).

$$dN = \frac{g(r)\cdot N\cdot 4\pi r^2 dr}{V} \tag{11}$$

In the formula, N is the number of B atoms and V is the volume of the model. Fig. 4 (B) shows the calculation results.

The number of H_W atoms around O_S atoms in C_{12} $(EO)_7$, C_{12} $(EO)_{15}$, and C_{12} $(EO)_{23}$ are 0.79, 0.53, and 0.45, respectively. The aggregation degree of water molecules around the ethoxy group decreases with the increase of the degree of ethoxylation. However, considering that there are 7, 15, and 23 ethoxy groups in C_{12} $(EO)_7$, C_{12} $(EO)_{15}$, and C_{12} $(EO)_{23}$, respectively, that is, the corresponding number of oxygen atoms. Then the calculation method of the number of H_W atoms around a single surfactant molecule is: the number of O_S in the surfactant molecule is multiplied by the coordination number of the O_S atom, and the calculated values are: 5.53, 7.95, and 10.35, respectively. The degree of water molecule aggregation around each surfactant molecule is still increased when the degree of ethoxylation rises. This result is in line with the diffusion cofficient analysis that was previously discussed. This is due to the fact that as n increases, the head groups of the surfactants become longer and are bent and intertwined to form a denser network layer, which allows the ethoxy groups to overlap. This agrees with the adsorption energy analysis's findings. However, in general, as the value of n rises, the degree of water molecule aggregation surrounding each surfactant molecule rises, increasing the capacity to attach to water molecules. The surface of the modified coal becomes more hydrophilic.

3.2.6. Number of hydrogen bonds

The variation in hydrophilicity between water and modified coal may be attributed to the different numbers of hydrogen bonds. The intermolecular hydrogen acceptor distance was less than 0.25 nm, and the donor hydrogen acceptor angle was larger than 135°, which were geometric criteria used to determine the existence of hydrogen bonds (Xu et al., 2014). The calculation results are shown in Table 4S.

Dodecyl polyoxyethylene surfactants significantly enhance the number of hydrogen bonds between the altered coal surface and water molecules, suggesting that these surfactants may boost the hydrophilicity of anthracite. And the rise in hydrophilicity to anthracite increases according to the degree of ethoxylation. This is in line with the diffusion cofficient and RDF analyses mentioned above.

4. Conclusions

Surface tension tests and HLB calculations show that the surfactants'

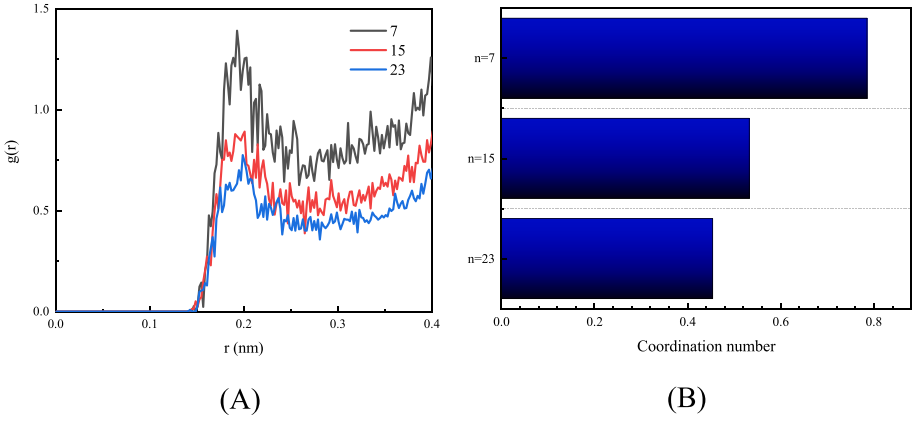

Fig. 4. The RDF and coordination number between O_S and H_W (A) RDF; (B) coordination number.

hydrophilicity increases with increasing ethoxylation levels. Contact angle experiment, XPS and FTIR tests demonstrate that the hydrophilicity rises as the ethoxylation degree rises after the surfactant's adsorption to anthracite. Relative concentration distribution study reveals that the hydrophilic headgroups are more consistently distributed over the whole distribution range with increasing ethoxylation degree. The hydrophobic tail chain is driven to be uniformly distributed along with the uniform distribution of the hydrophilic head group as the contact between the hydrophilic head group and water intensifies and eventually takes control. It is discovered using diffusion cofficient and RDF analysis that the addition of polyoxyethylene ether nonionic surfactants enhances the degree of hydrophilicity on the surface of anthracite, and the greater the degree of ethoxylation, the more powerfully the modified coal surface can bind to water molecules. By counting the amount of hydrogen bonds, it was discovered that after adhering to the anthracite, the polyoxyethylene ether surfactants created more hydrogen bonds with water, making the anthracite's surface hydrophilic.

Credit author statement

Xuanlai Chen: Methodology, Investigation, Project administration, Writing - original draft. **Guochao Yan:** Supervision, Funding acquisition, Writing - review & editing. **You Zhou:** Funding acquisition, Writing - review & editing. **Guang Xu:** Writing - review & editing. **Xuyang Bai:** Formal analysis. **Jiajun Li:** Formal analysis.

Declaration of competing interest

The authors declare that they have no known competing financial interests or personal relationships that could have appeared to influence the work reported in this paper.

Data availability

The data that has been used is confidential.

Acknowledgements

This work was supported by the National Natural Science Foundation of China (Grant No.51974195); the National Natural Science Foundation of China (Grant No. 52104283); the Natural Science Foundation of Hunan Province of China (Grant No. 2021JJ40779); the UWA-China Joint Scholarships, and the China Scholarship Council (CSC No. 202106930014).

Appendix A. Supplementary data

Supplementary data to this article can be found online at https://doi.org/10.1016/j.chemosphere.2022.136902.

References

Anvari, M.H., Liu, Q.X., Xu, Z.H., Choi, P., 2018. Molecular dynamics study of hydrophilic sphalerite (110) surface as modified by normal and branched butylthiols. Langmuir 34, 3363–3373.
Chang, P., Zhao, Z.D., Xu, G., Ghosh, A., Huang, J.X., Yang, T., 2020. Evaluation of the coal dust suppression efficiency of different surfactants: a factorial experiment. Colloid. Surface. 595.
Chen, B., Wei, X.Y., Zong, Z.M., Yang, Z.S., Qing, Y., Liu, C., 2011. Difference in chemical composition of supercritical methanolysis products between two lignites. Appl. Energy 88, 4570–4576.
Chen, Z.R., Qiu, H.X., Hong, Z.X., Wang, G.H., 2020. Molecular dynamics simulation of a lignite structure simplified model absorbing water. Mol. Simulat. 46, 71–81.
Guo, J.Y., Zhang, L., Liu, S.Y., Li, B., 2018. Effects of hydrophilic groups of nonionic surfactants on the wettability of lignite surface: molecular dynamics simulation and experimental study. Fuel 231, 449–457.
He, X., Guvench, O., MacKerell Jr., A.D., Klein, M.L., 2010. Atomistic simulation study of linear alkylbenzene sulfonates at the water/air interface. J. Phys. Chem. B 114, 9787–9794.
Li, B., Guo, J.Y., Albijanic, B., Liu, S.Y., Zhang, L., Sun, X.L., 2020a. Understanding flotation mechanism of nonionic surfactants with different polarity on kaolinite as a gangue mineral: an experimental and simulation study. Miner. Eng. 148.
Li, B., Guo, J.Y., Liu, S.Y., Albijanic, B., Zhang, L., Sun, X.L., 2020b. Molecular insight into the mechanism of benzene ring in nonionic surfactants on low-rank coal floatability. J. Mol. Liq. 302.
Li, B., Liu, S.Y., Fan, M.Q., Zhang, L., 2019. The effect of ethylene oxide groups in dodecyl ethoxyl ethers on low rank coal flotation: an experimental study and simulation. Powder Technol. 344, 684–692.
Li, J., Han, Y., Qu, G.M., Cheng, J.C., Xue, C.L., Gao, X., Sun, T., Ding, W., 2017. Molecular dynamics simulation of the aggregation behavior of N-Dodecyl-N, N-Dimethyl-3-Ammonio-1-Propanesulfonate/sodium dodecyl benzene sulfonate surfactant mixed system at oil/water interface. Colloid. Surface. 531, 73–80.
Li, L., He, M., Li, Z.H., Ma, C.D., Yu, H., You, X.F., 2021. Wettability effect of ethoxylated nonyl phenol with different ethylene oxide chain length on Shendong long-flame coal surface. Mater. Today Commun. 26.
Lin, J., Wang, W., Bai, W.L., Zhu, M.N., Zheng, C., Liu, Z.L., Cai, X.F., Lu, D.D., Qiao, Z. W., Chen, F.Q., et al., 2017. A gemini-type superspreader: synthesis, spreading behavior and superspreading mechanism. Chem. Eng. J. 315, 262–273.
Liu, X.Y., Liu, S.Y., Cheng, Y.C., Xu, G.J., 2020a. Decrease in hydrophilicity and moisture readsorption of lignite: effects of surfactant structure. Fuel 273.
Liu, X.Y., Liu, S.Y., Fan, M.Q., Guo, J.Y., Li, B., 2018. Decrease in hydrophilicity and moisture readsorption of Manglai lignite using lauryl polyoxyethylene ether: effects of the HLB and coverage on functional groups and pores. Fuel Process. Technol. 174, 33–40.
Liu, Z.Q., Zhou, G., Li, S.L., Wang, C.M., Liu, R.L., Jiang, W.J., 2020b. Molecular dynamics simulation and experimental characterization of anionic surfactant: influence on wettability of low-rank coal. Fuel 279.
Lyu, S.F., Chen, X.J., Shah, S.M., Wu, X.M., 2019. Experimental study of influence of natural surfactant soybean phospholipid on wettability of high-rank coal. Fuel 239, 1–12.
Mishra, S.K., Panda, D., 2005. Studies on the adsorption of Brij-35 and CTAB at the coal-water interface. J. Colloid Interface Sci. 283, 294–299.
Ni, G.H., Li, Z., Sun, Q., Li, S., Dong, K., 2019a. Effects of [Bmim][Cl] ionic liquid with different concentrations on the functional groups and wettability of coal. Adv. Powder Technol. 30, 610–624.
Ni, G.H., Qian, S., Meng, X., Hui, W., Xu, Y.H., Cheng, W.M., Gang, W., 2019b. Effect of NaCl-SDS compound solution on the wettability and functional groups of coal. Fuel 257.
Pan, C.X., Wei, X.Y., Shui, H.F., Wang, Z.C., Gao, J., Wei, C., Cao, X.Z., Zong, Z.M., 2013. Investigation on the macromolecular network structure of Xianfeng lignite by a new two-step depolymerization. Fuel 109, 49–53.
Rodriguez-Abreu, C., 2019. On the relationships between the hydrophilic-lipophilic balance and the nanoarchitecture of nonionic surfactant systems. J. Surfactants Deterg. 22, 1001–1010.
Xia, Y.C., Yang, Z.L., Zhang, R., Xing, Y.W., Gui, X.H., 2019. Enhancement of the surface hydrophobicity of low-rank coal by adsorbing DTAB: an experimental and molecular dynamics simulation study. Fuel 239, 145–152.
Xu, C.H., Wang, D.M., Wang, H.T., Ma, L.Y., Zhu, X.L., Zhu, Y.F., Zhang, Y., Liu, F.M., 2019. Experimental investigation of coal dust wetting ability of anionic surfactants with different structures. Process Saf Environ 121, 69–76.
Xu, G., Chen, Y.P., Eksteen, J., Xu, J.L., 2018. Surfactant-aided coal dust suppression: a review of evaluation methods and influencing factors. Sci. Total Environ. 639, 1060–1076.
Xu, Y., Liu, Y.L., Gao, S., Jiang, Z.W., Su, D., Liu, G.S., 2014. Monolayer adsorption of dodecylamine Surfactants at the mica/water interface. Chem. Eng. Sci. 114, 58–69.
Yan, G.C., Ren, G., Bai, L.J., Feng, J.P., Zhang, Z.Q., 2020. Molecular model construction and evaluation of Jincheng anthracite. ACS Omega 5, 10663–10670.
Yan, H., Guo, X.L., Yuan, S.L., Liu, C.B., 2011. Molecular dynamics study of the effect of calcium ions on the monolayer of SDC and SDSn surfactants at the vapor/liquid interface. Langmuir 27, 5762–5771.
Yang, J.S., Yang, C.L., Wang, M.S., Chen, B.D., Ma, X.G., 2011. Crystallization of alkane melts induced by carbon nanotubes and graphene nanosheets: a molecular dynamics simulation study. Phys. Chem. Chem. Phys. 13, 15476–15482.
Yao, Q.G., Xu, C.C., Zhang, Y.S., Zhou, G., Zhang, S.C., Wang, D., 2017. Micromechanism of coal dust wettability and its effect on the selection and development of dust suppressants. Process Saf Environ 111, 726–732.
You, X.F., He, M., Zhang, W., Wei, H.B., Lyu, X.J., He, Q., Li, L., 2018. Molecular dynamics simulations of nonylphenol ethoxylate on the Hatcher model of subbituminous coal surface. Powder Technol. 332, 323–330.
You, X.F., He, M., Zhu, X.C., Wei, H.B., Cao, X.Q., Wang, P., Li, L., 2019. Influence of surfactant for improving dewatering of brown coal: a comparative experimental and MD simulation study. Separ. Purif. Technol. 210, 473–478.
Yuan, M.Y., Nie, W., Zhou, W.W., Yan, J.Y., Bao, Q., Guo, C.J., Tong, P., Zhang, H.H., Guo, L.D., 2020. Determining the effect of the non-ionic surfactant AEO(9) on lignite adsorption and wetting via molecular dynamics (MD) simulation and experiment comparisons. Fuel 278.
Zhang, L., Li, B., Xia, Y.C., Liu, S.Y., 2017. Wettability modification of Wender lignite by adsorption of dodecyl poly ethoxylated surfactants with different degree of ethoxylation: a molecular dynamics simulation study. J. Mol. Graph. Model. 76, 106–117.

Zhang, R., Xing, Y.W., Xia, Y.C., Luo, J.Q., Tan, J.L., Rong, G.Q., Gui, X.H., 2020. New insight into surface wetting of coal with varying coalification degree: an experimental and molecular dynamics simulation study. Appl. Surf. Sci. 511.

Zhao, T.T., Xu, G.Y., Yuan, S.L., Chen, Y.J., Yan, H., 2010. Molecular dynamics study of alkyl benzene sulfonate at air/water interface: effect of inorganic salts. J. Phys. Chem. B 114, 5025–5033.

Zhou, Q., Qin, B.T., 2021. Coal dust suppression based on water mediums: a review of technologies and influencing factors. Fuel 302.